

Oil & Natural Gas Technology

DOE Award No.: DE-FC26-06NT43067

Quarterly Progress Report (April – June 2008)

Mechanisms Leading to Co-Existence of Gas and Hydrate in Ocean Sediments

Submitted by:

The University of Texas at Austin
1 University Station C0300
Austin, TX 78712-0228

Prepared for:

United States Department of Energy
National Energy Technology Laboratory

August 4, 2008



Office of Fossil Energy

MECHANISMS LEADING TO CO-EXISTENCE OF GAS AND HYDRATE IN
OCEAN SEDIMENTS

CONTRACT NO. DE-FC26-06NT43067

QUARTERLY PROGRESS REPORT
Reporting Period: 1 Apr 08 – 30 Jun 08

Prepared by

Steven L. Bryant

Department of Petroleum and Geosystems Engineering
The University of Texas at Austin
1 University Station C0300
Austin, TX 78712-0228
Phone: (512) 471 3250
Email: steven_bryant@mail.utexas.edu

Ruben Juanes

Department of Civil and Environmental Engineering
Massachusetts Institute of Technology
77 Massachusetts Avenue, Room 48-319
Cambridge, MA 02139
Phone: (617)253-7191
Email: juanes@mit.edu

Prepared for

U.S. Department of Energy - NETL
3610 Collins Ferry Road
P.O. Box 880
Morgantown, WV 26508

Summary

Work during this quarter continued on discrete element modeling (DEM) coupling of fluid flow and sediment mechanics when two fluid phases are present, and of the critical curvatures for imbibition in the model sediments created in previous Tasks.

Our DEM work during this period has focused on the validation of the model with laboratory data, and the application of the model to the prediction of the mode of methane gas migration into the Hydrate Stability Zone (HSZ). The model accounts rigorously for the presence of two fluids in the pore space by incorporating grain forces due to pore fluid pressures, and surface tension between fluids. We elucidate the way in which gas migration may take place: (1) by capillary invasion in a rigid-like medium; and (2) by initiation and propagation of a fracture. We find that the main factor controlling the mode of gas transport in the sediment is the grain size, and show that coarse-grain sediments favor capillary invasion, whereas fracturing dominates in fine-grain media. The results have important implications for understanding hydrates in natural systems.

We discovered a simplified estimate of the critical curvature for imbibition of pores. The estimate is based on physical insight from applying the level set method (LSM) to the movement of menisci in individual pores. The Melrose criterion for an imbibition event implies that a pore can imbibe at several different curvatures, depending on which pair of gas/water interfaces merge within the pore. The largest of these curvatures corresponds to the situation when interfaces in two pore throats merge. This curvature is strongly correlated to the classical Haines estimate for imbibition. Thus we were able to find a useful empirical relationship between the rigorously obtained value and the Haines estimate. This will be useful in network simulations of imbibition (water displacing gas from a sediment) following drainage.

The final reports for Task 4 (Fracture initiation and propagation) and Subtask 5.1 (Compute critical curvatures for pore-level events) were submitted to DOE during this reporting period.

One paper was presented at the Offshore Technology Conference in Houston in May 2008. Two papers were written, and corresponding posters presented at the International Conference on Gas Hydrates in Vancouver in July 2008. A paper to be presented at the Society of Petroleum Engineers Annual Technical Conference and Exhibition (Sept. 2008) was completed.

Activities in This Reporting Period

Task 4.0 – Fracture Initiation and Propagation

Subtask 4.1. Initialize the model

This task has been completed, and reported upon in previous communications.

Subtask 4.2. Poromechanics with a single-fluid system

This task has been completed, and reported upon in previous communications. However, we have extended our validation of the model. As an example of this additional validation effort, we show below the results for the simulated fluid–solid behavior during undrained consolidation tests. During the undrained compaction process, the vertical strain ε , total vertical stress σ , and average pore pressure p are recorded. In view of the effective stress concept, the total stress required to achieve a given deformation in a fluid-saturated medium is larger than for a dry medium. In the realm of the linear theory of poroelasticity, the effective stress is given by:

$$\sigma' = \sigma - bp,$$

where b is the Biot coefficient. The dependence of the Biot coefficient on the solid and fluid properties of the constituents is reasonably well understood. The Biot coefficient approaches a value of one only in the limit of incompressible grains. If the grain and fluid compressibilities are comparable, the Biot coefficient is less than one.

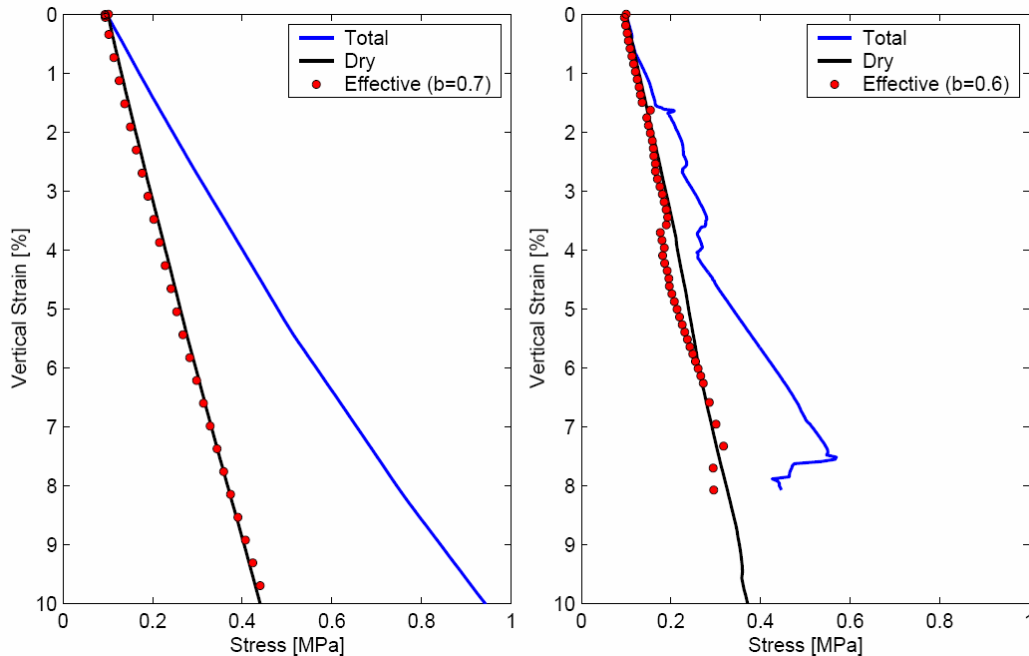


Figure 1. Stress–strain curves for uniaxial undrained compaction. Left: cemented/cohesive sample. Right: unconsolidated/cohesionless sample.

In Figure 1 we show the stress-strain curves for a cemented/cohesive sample (left figure), and for an unconsolidated/cohesionless sample (right figure). In both cases, we plot the stress-strain curves for the fluid-saturated medium (total stress), and for a dry medium. We confirm that the dry stress curve can be interpreted as the effective stress, and recovered by subtracting the pore pressure times the Biot coefficient from the total stress. In this way, the Biot coefficient can be inferred. Figure 1 illustrates the proper behavior of the coupled DEM model in two ways: (1) the results are in agreement with the Biot theory of poroelasticity (at least in the region of small strains); and (2) the values of b inferred from the simulation also agree well with experimental values.

Subtask 4.3. Hydraulic fracturing with an elastic membrane representation of a two-fluid system

In the final report for Task 4 we suggest re-naming this Subtask 4.3: “Microporomechanics of two-fluid systems”, because we have been able to relax the initial assumption of an “elastic membrane” model, and develop a model that incorporates (even if in a simplified fashion) the effect of adhesive forces due to surface tension between brine and methane gas.

The objective of this subtask is to investigate under which conditions the material will “fracture” due to the invading methane gas phase. Migration of a gas phase through a deformable medium may occur by two end-member mechanisms: (1) capillary invasion through a rigid medium, and (2) fracture opening.

In previous progress reports we showed that the model is able to capture the fracturing phenomenon. If the gas cannot invade a throat by capillarity, the gas pressure will act to separate the grains. When the bond between two grains is lost, and the gap between them increases sufficiently, the gas-water interface advances and a new pore is loaded with a higher pressure. We have also shown that one expects the development of vertical fractures that open up the sediment in the direction of minimum compressive stress (usually the horizontal stress).

Since the model is able to predict which one of the two end-member mechanisms for methane transport (sediment fracturing or capillary invasion) is dominant, we find that the most sensitive factor determining the favored mechanism is the grain size: fracturing is favored for fine-grained sediments, while capillary invasion is favored for coarse-grained sediments. In Figure 2 we show two snapshots of the evolution of the methane-water interface for a coarse-grain sediment of characteristic size $r_{\min} = 1$ mm. It is apparent that during the invasion of methane gas, there is virtually no movement of the solid grains: the sediment acts like a rigid skeleton. Indeed, the network of grain contact compressive forces remains the same during the process. Invasion of gas from pore to pore occurs when the gas pressure (minus the water pressure) exceeds the capillary entry pressure of the throat.

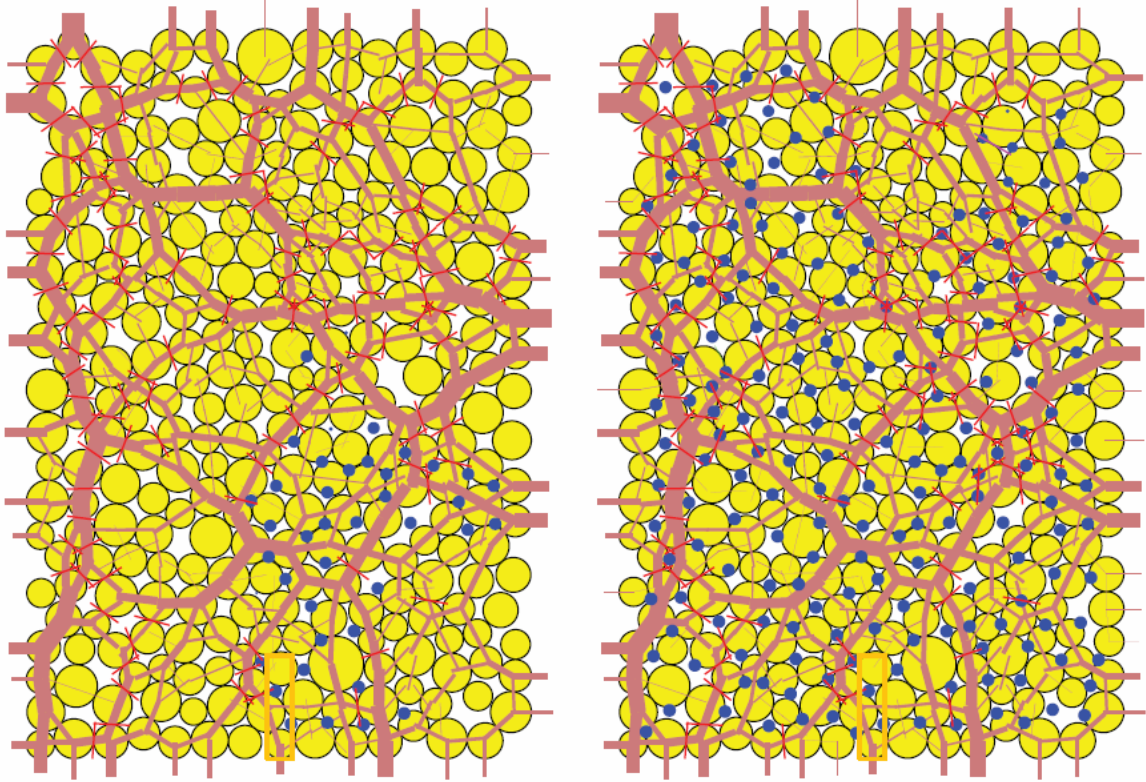


Figure 2. The case $r_{\min} = 1 \text{ mm}$. Methane invasion by capillary pressure.

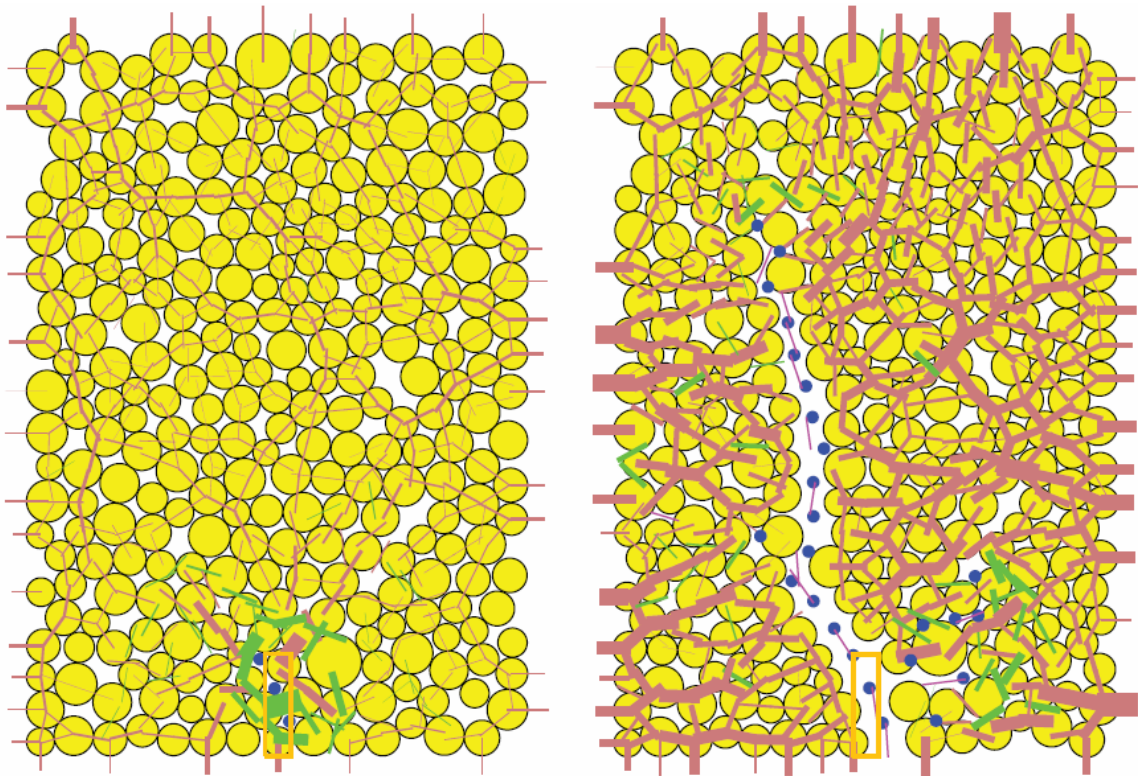


Figure 3. The case $r_{\min} = 1 \text{ }\mu\text{m}$. Methane invasion by fracture opening.

The behavior is completely different when a much smaller grain size is used. The evolution of the methane gas migration for $r_{\min} = 1 \mu\text{m}$ is shown in Figure 3. Mechanical effects become dominant, and the solid skeleton no longer behaves like a rigid medium. A fracture is created and propagates vertically.

We have started to synthesize this information to provide useful estimates of when the fracturing regime will be dominant in natural settings. The two main variables controlling the behavior are the lateral Earth stress (confining stress) and the grain size. In Figure 4, we summarize the result of simulations for an effective confining stress of 0.1 MPa, which corresponds to a sediment depth of about 10 meters. For large enough grain size, methane gas invades by capillarity. Therefore, the log-log plot of invasion pressure vs. grain size displays the characteristic slope of -1. For a small enough grain size (in the order of microns), there is a transition from capillary invasion to fracture formation. The pressure required for the methane gas to invade increases with decreasing grain size, but the relation between the two is no longer 1:1. This behavior reflects a combination of ductile material behavior and some stress concentration at the fracture tip.

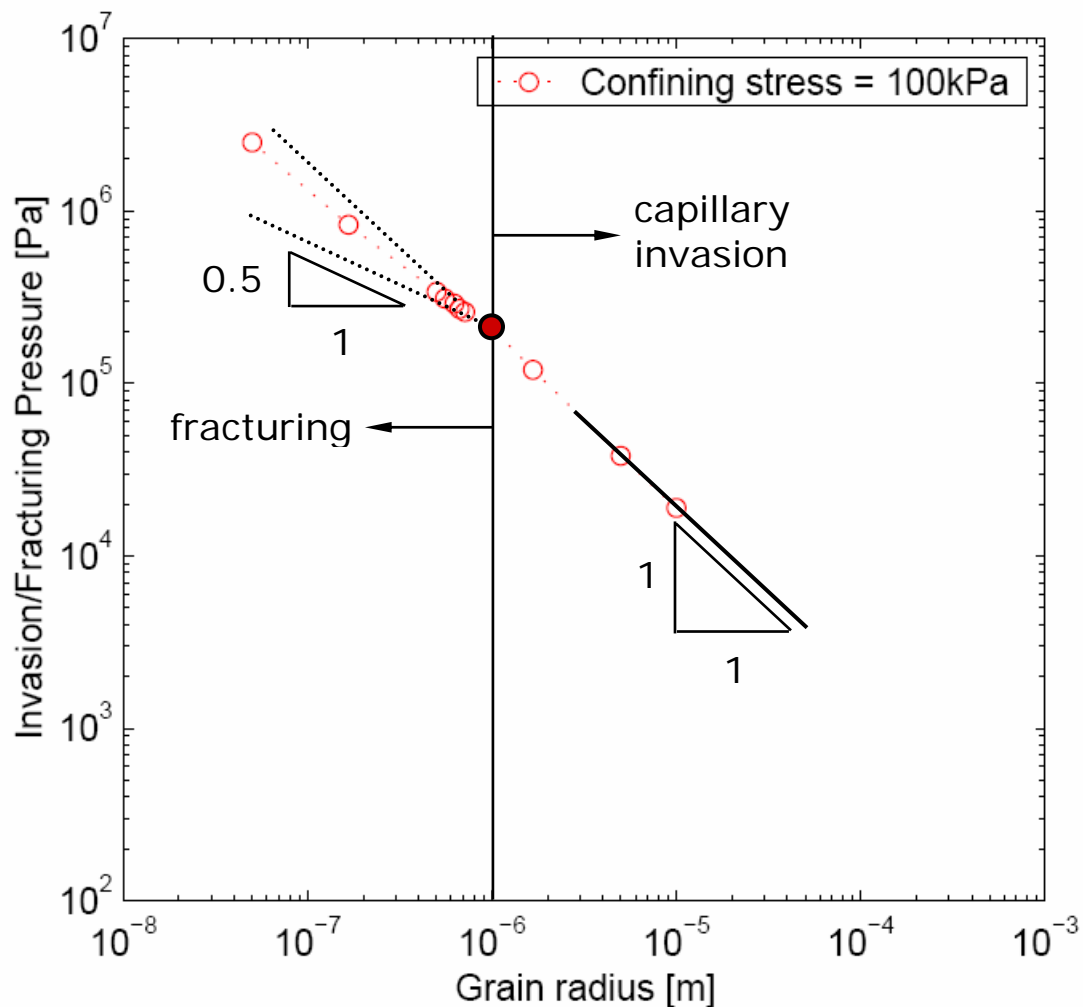


Figure 4. Invasion pressure vs. grain size, displaying transition from capillary invasion to fracturing. The critical grain size depends on the lateral Earth stresses.

Subtask 5.1. Compute critical curvatures for pore-level events

In the conceptual model being examined in this project, hydrate formation depends upon the location and geometry of the gas/water interface. We developed and produced a final draft catalog of critical curvatures for model sediments based on the results of this work.

For computing the imbibition curvature we use two of the geometric data files developed in Task 3:

Coordinates_PackingNN.txt
Tes_Matrix_PackNN.txt

where NN is the packing number, ranging from 1 to 76.

In the first type of data files are the coordinates of the spheres in each pack. The line number in the file corresponds to the index number of the sphere. There are 4 records in each line, which from left to right stores x coordinate, y coordinate, z coordinate and the sphere radius of the corresponding sphere, respectively.

In the second type of the data files are the sphere indices of the tetrahedra generated by using Delaunay tessellation. Each row corresponds to one tetrahedron, and the 4 numbers are the indices of the spheres that define this tetrahedron. The line number of the file is the index of the tetrahedron. The void space within each tetrahedron corresponds to a pore body.

In each tetrahedron, there may be an inscribed sphere, that is, a sphere that is tangent to all 4 spheres defining the tetrahedron. The radius of this so-called insphere can be used to calculate the imbibition curvature based on Mellor's theory.

The first step is to compute the insphere radii for the pores in each pack. The computation is based on the following nonlinear equation system:

$$\begin{aligned}(x_{inscribed} - x_1)^2 + (y_{inscribed} - y_1)^2 + (z_{inscribed} - z_1)^2 &= (r_{inscribed} + r_1)^2 \\(x_{inscribed} - x_2)^2 + (y_{inscribed} - y_2)^2 + (z_{inscribed} - z_2)^2 &= (r_{inscribed} + r_2)^2 \\(x_{inscribed} - x_3)^2 + (y_{inscribed} - y_3)^2 + (z_{inscribed} - z_3)^2 &= (r_{inscribed} + r_3)^2 \\(x_{inscribed} - x_4)^2 + (y_{inscribed} - y_4)^2 + (z_{inscribed} - z_4)^2 &= (r_{inscribed} + r_4)^2\end{aligned}\tag{1}$$

where $(x_{inscribed}, y_{inscribed}, z_{inscribed}, r_{inscribed})$ are the coordinates and radius of the inscribed sphere, and (x_i, y_i, z_i, r_i) are the coordinates and radii of the spheres forming the tetrahedron, where i ranges from 1 to 4.

We solve the above nonlinear equation system numerically. Iteration is a powerful tool to deal with this kind of problem. A relaxation factor of 2/3 was used to stabilize the solution and a maximum iteration count of 10,000 was imposed.

The results showed that in some tetrahedra, there were no inscribed inspheres. This happens in some kinds of specific geometry. Examples include when 4 spheres have similar radii and their centers lie almost on a plane (Figure 1), and when a very big sphere is surrounded by 3 smaller spheres (Figure 2). The possibility of not finding inscribed sphere increases as the packing gets worse sorted. For the well sorted packing (e.g. packing 1), this situation only happened around 10 times in our calculation; however in the less well sorted packings (e.g. packing 19), the situation happens thousands of times.

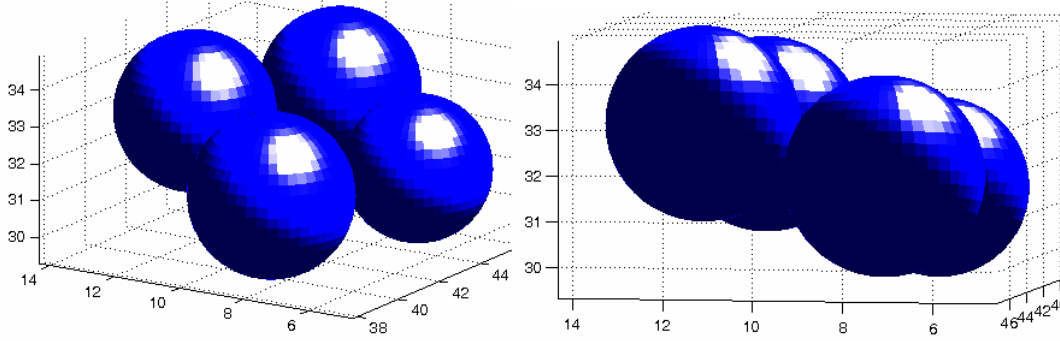


Figure 1, A pore (Delaunay tetrahedron) for which an inscribed sphere does not exist. The left and right figures show the same pore from different points of view.

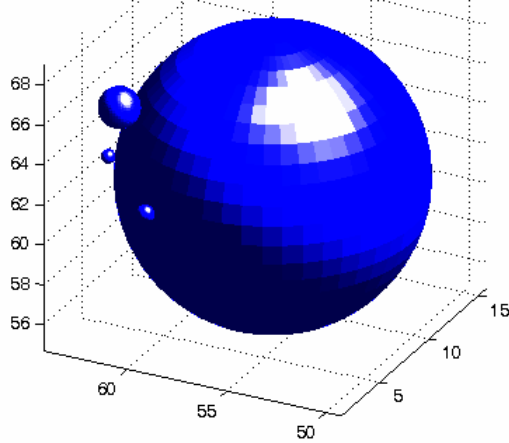


Figure 2, A pore (Delaunay tetrahedron) formed by one large sphere and three smaller spheres. No inscribed sphere exists for this pore.

The estimate of dimensionless imbibition curvature due to Mason and Mellor:

$$C_{imb}^* = \frac{2R_{avg}}{r_{inscribed}} - 1.6 \quad (2)$$

where R_{avg} is the average radius of spheres in the packing. This equation was derived from monodisperse sphere pack. The constant -1.6 is introduced in the equation in order to preserve the imbibition hysteresis. However, as it was originally developed from the monodisperse pack, this equation cannot be generalized to packings with sufficiently broad distribution of sphere radii. We have therefore developed a modified equation using insights gained from application of the level set method.

Prodanović and Bryant^[2] developed a novel way to calculate the imbibition curvature by using Level Set Method. All pores can have a multiplicity of imbibition curvatures, depending on which menisci and/or pendular rings merge to trigger the imbibition event.

For a given pore, the largest curvature of these curvatures, and therefore the curvature most likely to apply during an imbibition process, is found when menisci in two throats merge. The merger of menisci is physically and geometrically analogous to Haines' original concept, namely, that a pore imbibed when the gas/water meniscus forms a sphere contained within the pore. Consequently there is a strong correlation between this curvature and the Haines' estimate of $C_{imb}^* = \frac{2R_{avg}}{r_{inscribed}}$. For a monodisperse packing, the imbibition curvatures, which are dependable, can be approximately fit by the following equation:

$$C_{imb}^* = \frac{1.25R_{avg}}{r_{inscribed}} + 0.8 \quad (3)$$

Equation (3) eliminates the possibility of negative imbibition curvatures and is simple to use.

National Energy Technology Laboratory

626 Cochrans Mill Road
P.O. Box 10940
Pittsburgh, PA 15236-0940

3610 Collins Ferry Road
P.O. Box 880
Morgantown, WV 26507-0880

One West Third Street, Suite 1400
Tulsa, OK 74103-3519

1450 Queen Avenue SW
Albany, OR 97321-2198

2175 University Ave. South
Suite 201
Fairbanks, AK 99709

Visit the NETL website at:
www.netl.doe.gov

Customer Service:
1-800-553-7681

